Synthesis and Characterization of VPI-5 Supported TiO_2 Clusters

Robert J. Davis

Department of Chemical Engineering, University of Virginia, Charlottesville, Virginia 22903-2442

Received June 19, 1992. Revised Manuscript Received September 30, 1992

Titania clusters were prepared by impregnation, hydrolysis, and calcination of a metal alkoxide precursor inside the channels of aluminophosphate molecular sieve VPI-5. The new material was characterized by X-ray diffraction, ultraviolet reflectance spectroscopy, laser Raman spectroscopy, transmission electron microscopy, and energy-dispersive X-ray analysis. Results from these techniques suggest that the titania clusters are located inside the channels of the molecular sieve support. However, the optical properties and crystal structure differ from those of bulk reference materials. For titania in VPI-5, the bandgap energy measured by UV reflectance spectroscopy is about 0.3 eV greater than bulk-phase anatase, and the Raman peaks are shifted to higher wavenumbers than those of anatase, indicating that titania is present as nanometer-sized, substoichiometric clusters. Additionally, TEM and EDX analyses reveal an inhomogeneous distribution of titania throughout the sample.

Introduction

Isolated, nanophase semiconductors can be considered as zero- and one-dimensional quantum dots and quantum wires. Therefore, interest in using these systems as device components in quantum electronics and nonlinear optics is rapidly growing. However, stabilizing the formation of semiconductor clusters having diameters near 1 nm remains a significant challenge. The materials synthesis, quantum size effects, and photophysical properties of nanometer-sized clusters have been recently reviewed.[1] One way to prepare small semiconductor clusters is to form them inside a zeolite framework. For example, the structure and optical properties of CdS clusters in zeolites A, X, and Y[2,3] and the optical properties of PbS in zeolite Y[3] were investigated to better understand the differences between bulk semiconductor properties and those of molecular units or small clusters. In addition, NMR spectroscopy, luminescence quenching, and infrared spectroscopy have been used to study the structure and properties of Tl^+ loaded into zeolite Y.[4] Other semiconductor systems recently investigated include CdSe in zeolites A, X, and mordenite[5] and GaP in zeolite Y.[6] Advances in the area of zeolite inclusion phenomena prompted Ozin and Özkar to propose the term "zeolite topotaxy", relating concepts of intrazeolitic guest–host chemistry to the more familiar concept of epitaxy on two-dimensional surfaces.[7]

One method used to prepare zeolite-supported semiconductors is ion exchange. Cations in the host zeolite framework are replaced by desired precursor cations which are subsequently converted to the semiconductor phase after chemical or thermal treatment. However, large electric field gradients exist in zeolite materials due to the negative charges of the aluminosilicate framework and the positive charges of mobile cations. Therefore, the electronic (and catalytic) properties of clusters in microporous materials without large electric field gradients may be different from those of clusters in aluminosilicate zeolites. Aluminophosphate molecular sieves are neutral framework materials containing no exchangeable cations. Thus, aluminophosphate molecular sieves are useful materials for studying the influence of framework composition on the properties of supported clusters. In fact, a recent study of the catalytic reactions of *n*-hexane over Pt metal clusters revealed that the product distributions from Pt clusters supported inside aluminophosphate molecular sieves were very different from the product distributions from Pt-containing aluminosilicate and silicate materials, indicating that the support significantly influences Pt-catalyzed reactions.[8,9]

In this paper, the synthesis of nanometer-sized TiO_2 semiconductor clusters inside the unidimensional channels of aluminophosphate molecular sieve VPI-5 is described. Since no exchangeable cations are present in VPI-5, ion-exchange methods for loading titania into the support are not applicable. Therefore, a liquid-phase impregnation procedure was used to load a titanium precursor into the VPI-5 channel structure. The oxide semiconductor phase was then generated inside the channels by chemical reaction of the precursor-loaded VPI-5. Liquid-phase impregnation techniques have been shown recently to produce extremely well dispersed platinum clusters, containing 5–6 atoms/cluster, inside the unidimensional channels of zeolite L.[10] Whether these techniques are applicable to forming nanometer-sized TiO_2 clusters is investigated here.

Several novel applications for titanium zeolites have been described recently. For example, zeolites containing titanium dioxide have been prepared as molecular assemblies for artificial photosynthesis.[11,12] Also, TiO_2/zeolites catalyze selective oxidation of alkenes[13] and photocatalytic

(1) Wang, Y.; Herron, N. *J. Phys. Chem.* **1991**, *95*, 525.
(2) Herron, N.; Wang, Y.; Eddy, M. M.; Stucky, G. D.; Cox, D. E.; Moller, K.; Bein, T. *J. Am. Chem. Soc.* **1989**, *111*, 530.
(3) Wang, Y.; Herron, N. *J. Phys. Chem.* **1987**, *91*, 257.
(4) McMurray, L.; Holmes, A. J.; Kuperman, A.; Ozin, G. A.; Özkar, S. *J. Phys. Chem.* **1991**, *95*, 9448.
(5) Miyazaki, S.; Iwakura, C.; Yoneyama, H. *Denki Kagaku* **1989**, *57*, 1168.
(6) MacDougall, J. E.; Eckert, H.; Stucky, G. D.; Herron, N.; Wang, Y.; Moller, K.; Bein, T.; Cox, D. *J. Am. Chem. Soc.* **1989**, *111*, 8006.
(7) Ozin, G. A.; Özkar, S. *Adv. Mater.* **1992**, *4*, 11.
(8) Mielczarski, E.; Hong, S. B.; Davis, M. E. *J. Catal.* **1992**, *134*, 370.
(9) Mielczarski, E.; Hong, S. B.; Davis, R. J.; Davis, M. E. *J. Catal.* **1992**, *134*, 359.
(10) Miller, J. T.; Sajkowski, D. J.; Modica, F. S.; Lane, G. S.; Gates, B. C.; Vaarkamp, M.; Grondelle, J. V.; Koningsberger, D. C. *Catal. Lett.* **1990**, *6*, 369.
(11) Krueger, J. S.; Lai, C.; Li, Z.; Mayer, J. E.; Mallouk, T. E. in *Inclusion Phenomena and Molecular Recognition*; Atwood, J., Ed.; Plenum Press: New York, 1990; p 365.
(12) Kim, Y. I.; Riley, R. L.; Huq, M. J.; Salim, S.; Le, A. N.; Mallouk, T. E. *Mater. Res. Soc. Symp. Proc.* **1991**, *233*, 145.

0897-4756/92/2804-1410$03.00/0

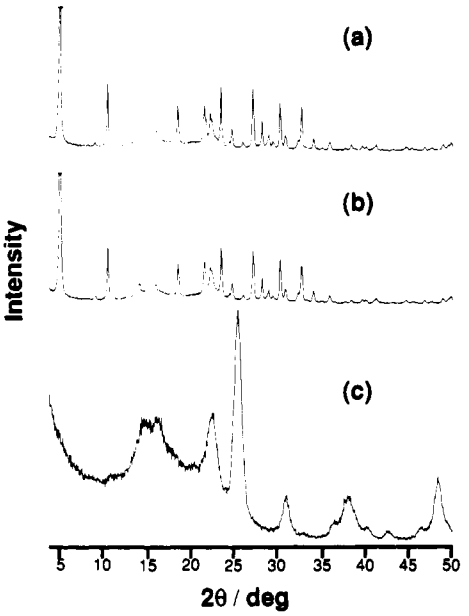

Figure 1. X-ray powder diffraction patterns of titania samples: (a) Ti impregnated VPI-5, hydrolyzed in water; (b) sample in (a) after calcination in vacuum at 673 K for 4 h; (c) anatase powder prepared by hydrolysis of titanium isopropoxide and calcination at 673 K for 4 h.

oxidation of nitrous anions.[14]

Experimental Methods

Sample Preparation. The aluminophosphate molecular sieve VPI-5 was synthesized according to methods described previously.[15] The following steps were taken to support titania crystallites on the molecular sieve. First, about 2 g of VPI-5 was evacuated at room temperature for 7 h to dehydrate the sample. After backfilling the cell with Ar, a 1:1 mixture of titanium isopropoxide (Aldrich, 97%) and 2-propanol (Fisher, 99.9%) was added dropwise to the dried VPI-5 to the point of incipient wetness. The impregnated sample was then evacuated for 15 min at room temperatures to partially remove the 2-propanol. Next, the powder was added to 400 mL of distilled, deionized water and stirred at 323 K for 45 h to hydrolyze the supported titanium isopropoxide. A portion of the filtered, dried sample was evacuated at room temperatures overnight and then rapidly heated in vacuum to 673 K and maintained at that temperature for 4 h. Afterward, the sample was cooled in vacuo and exposed to air. Elemental analysis performed by Galbraith Laboratories showed a final titanium content of 5.06 wt % Ti supported on VPI-5.

Two samples of TiO_2 were also prepared as reference materials. First, titanium isopropoxide was hydrolyzed in water at the same conditions described above for the molecular sieve sample. A portion of the filtered, dried precipitate was calcined in air at 673 K for 4 h, forming the anatase phase of TiO_2. A second portion of the precipitate was calcined in air at 1073 K for 4 h, forming the rutile phase of TiO_2. Specific surface areas of the anatase and rutile powders were measured by the single-point BET method and were found to be 91 and 2 $m^2 g^{-1}$, respectively.

Sample Characterization. The titania samples were examined with several techniques. X-ray diffraction patterns were recorded on a Scintag diffractometer operating with a Cu Kα X-ray source. A Shimadzu UV–vis spectrophotometer was used to record the ultraviolet reflectance spectra of the various samples directly in air with no pretreatment. In addition, laser Raman spectroscopy was performed using a Nicolet System 800 FT-IR and FT Raman accessory with a Nd:YAG laser powered at 1 W in the near-IR (9394 cm^{-1}). The number of scans were varied from 100 to 1500 depending on the observed signal-to-noise ratio. Transmission electron microscopy and energy-dispersive analysis of the emitted characteristic X-rays (EDX) were performed on a Philips electron microscope outfitted with a KeVex solid-state detector.

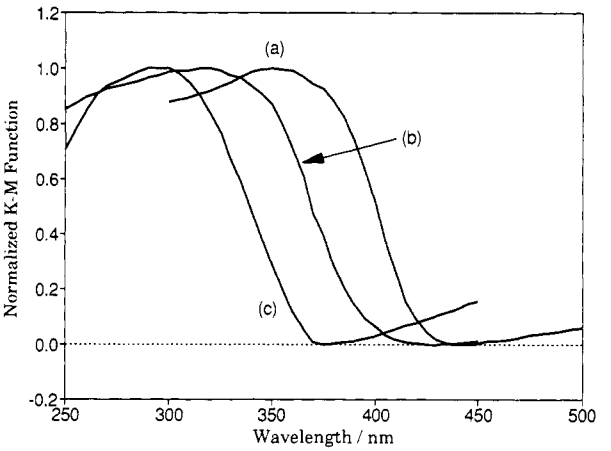

Figure 2. Normalized Kubelka–Munk functions derived from UV reflectance spectroscopy of titania samples: (a) rutile powder; (b) anatase powder; (c) TiO_2/VPI-5 after calcination at 673 K for 4 h.

Results

X-ray Diffraction. The X-ray diffraction patterns of the hydrolyzed, titanium-impregnated, VPI-5 samples before and after heating at 673 K are shown in parts a and b of Figure 1, respectively. For comparison, the X-ray pattern of bulk titania prepared by the same method is displayed in Figure 1c. One important result is that the aluminophosphate molecular sieve VPI-5 was found to be stable to the temperature used for the synthesis of the supported titania crystallites. The peaks in the X-ray diffraction pattern of hydrolyzed TiO_2/VPI-5 before heating (Figure 1a) are associated with VPI-5, and these peaks remain in the X-ray pattern of the same sample after heating to 673 K, demonstrating conclusively that the framework structure of the molecular sieve remains intact after calcination at high temperature.

Close examination of Figure 1 does not reveal any peaks associated with the titania clusters. The synthesis conditions used to prepare the calcined TiO_2/VPI-5 should produce titania clusters having the anatase crystal structure, the X-ray pattern of which is shown in Figure 1c. The lack of any titania phase detectable by X-ray diffraction is consistent with the formation of very small clusters located most probably in the framework of the molecular sieve. Indeed, if the titania clusters are located inside VPI-5 then the upper limit of the cluster size is 1.2 nm, the channel diameter of VPI-5, and clusters of this size are not expected to be detected by conventional X-ray diffraction methods. However, additional evidence for the size of the VPI-5-supported titania clusters is necessary.

Ultraviolet Reflectance Spectroscopy. Ultraviolet reflectance spectroscopy is often used to measure the bandgap energy of semiconductor materials. The reflectance spectra are shown in Figure 2 for the bulk titania samples of anatase and rutile and for the calcined titania-loaded VPI-5 sample. No structure in the region of interest is present in the reflectance spectrum of pure VPI-5 so the absorption thresholds in Figure 2 are attributed solely to the titania clusters. Direct bandgaps of these materials can be determined by plotting $(\alpha h\nu)^2$ versus excitation energy (where α is the absorption coefficient) and extrapolating the linear part of the curve to $(\alpha h\nu)^2 =$

(13) Tatsumi, T.; Nakamura, M.; Yuasa, K.; Tominaga, H. *Catal. Lett.* **1991**, *10*, 259.
(14) Yamagata, S.; Mineo, K.; Murao, N.; Ohta, S.; Mizoguchi, I. *Denki Kagaku* **1991**, *59*, 871.
(15) Davis, M. E.; Montes, C.; Garces, J. M. In *Zeolite Synthesis*; Occelli, M. L., Robson, H. E., Eds.; ACS Symp. Ser. 398; American Chemical Society: Washington, DC, 1989, p 291.

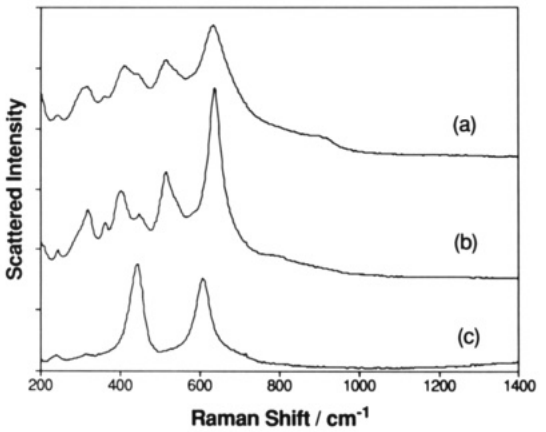

Figure 3. Laser Raman spectra of unsupported titania samples: (a) hydrolyzed titanium isopropoxide; (b) anatase powder; (c) rutile powder.

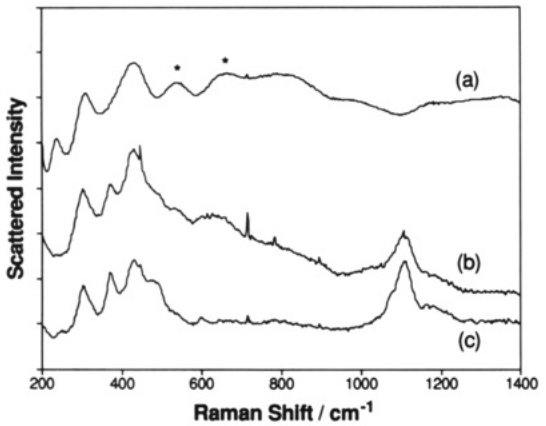

Figure 4. Laser Raman spectra of molecular sieve materials: (a) calcined TiO_2/VPI-5; (b) Ti impregnated VPI-5, hydrolyzed in water; (c) VPI-5.

0.[16] Bandgaps were estimated to be 3.05, 3.28, and 3.57 eV for rutile, anatase, and TiO_2/VPI-5, respectively. The bandgap for rutile is generally considered to be about 3.0 eV, while the bandgap for anatase is about 3.2–3.3 eV, and these compare well to the values found in this work. An interesting result is that the bandgap shift for TiO_2 inside the channels of VPI-5 as measured by the shift in the UV reflectance spectrum (30 nm) is an additional 0.3 eV larger than the value for anatase, indicating a bandgap energy near 3.6 eV.

Laser Raman Spectroscopy. The titania samples were also examined by laser Raman spectroscopy. The spectra in Figure 3 correspond to the Raman scattering from hydrolyzed titanium isopropoxide, anatase, and rutile bulk titania powders described earlier. The three prominent peaks at 639, 516, and 403 cm^{-1} in spectra (a) and (b) are characteristic of the anatase crystal structure.[17] Rutile has prominent peaks near 608 and 445 cm^{-1} which are present in spectrum (c).[17] The hydrolyzed alkoxide sample clearly shows the peaks associated with the anatase crystal structure, indicating that the precipitation conditions used in this study favor the formation of anatase at 323 K. This observation is consistent with the X-ray diffraction pattern of the material which shows broad peaks for anatase and no detectable rutile. Since the experimental conditions used to generate the materials represented in Figures 3a,b

(16) Bube, R. H. *Electronic Properties of Crystalline Solids—An Introduction to Fundamentals*; Academic Press: New York, 1974.
(17) Arsov, Lj D.; Kormann, C.; Plieth, W. *J. Raman Spectrosc.* **1991**, *22*, 573.

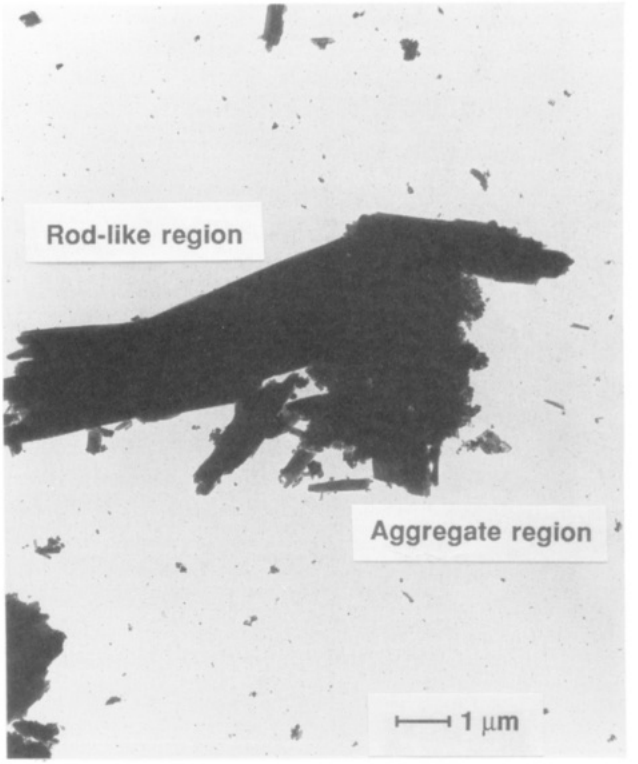

Figure 5. Transmission electron micrograph of Ti impregnated VPI-5, hydrolyzed in water.

are analogous to the hydrolysis and calcination conditions for the TiO_2/VPI-5 sample, anatase is the expected crystal structure of VPI-5 supported titania. Figure 4 compares the Raman spectra of calcined TiO_2/VPI-5 (a), hydrolyzed TiO_2/VPI-5 (b), and VPI-5 (c). The peaks in the spectrum of calcined TiO_2/VPI-5 at 432 and 310 cm^{-1} appear in all of the spectra and result from vibrations of the molecular sieve framework. Additional work with VPI-5 revealed that when the molecular sieve is dehydrated, a peak appears at 238 cm^{-1} which accounts for the lowest wavenumber peak in the spectrum of calcined TiO_2/VPI-5. If anatase was present in TiO_2/VPI-5, then some of the titania peaks would overlap the low-wavenumber peaks associated with the support. However, the two peaks in calcined TiO_2/VPI-5 at 541 and 670 cm^{-1} (indicated by asterisks) are apparently due to the supported TiO_2. The peak positions in the titania molecular sieve are shifted from the bulk-phase anatase values to higher wavenumbers by about 25–30 cm^{-1} and are completely different from the bulk-phase rutile peak positions.

Transmission Electron Microscopy. A transmission electron micrograph of hydrolyzed TiO_2/VPI-5 is shown in Figure 5. The micrograph shows two distinctly different types of material. The first type appears to be rodlike and crystalline while the second type, adjacent to the first, appears to be small crystalline aggregates or amorphous material. The difference in crystallinity between the two regions in the micrograph could not be determined since diffraction spots vanished within a second of exposure to the electron beam, precluding a precise correlation between location and crystallinity. Additional efforts to determine crystallinity and titania cluster size at higher magnification were also unsuccessful due to the instability of VPI-5 in the electron beam and the lack of significant contrast between titania and VPI-5.

The electron beam was narrowly focused thus enabling EDX spectroscopy to determine the elemental composition of the two different sample regions in Figure 5. The EDX spectra for both the rodlike region and the aggregate region

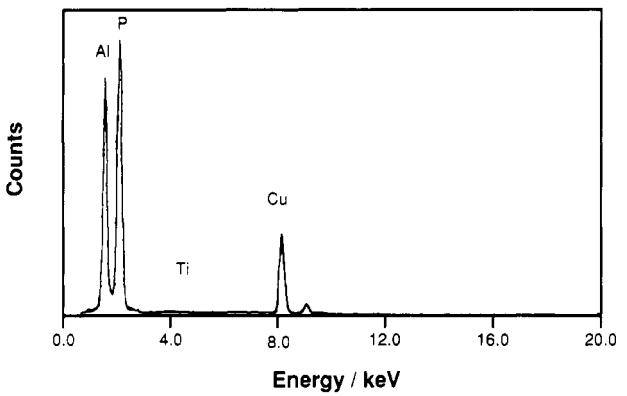

Figure 6. EDX spectrum of rodlike region of micrograph in Figure 5.

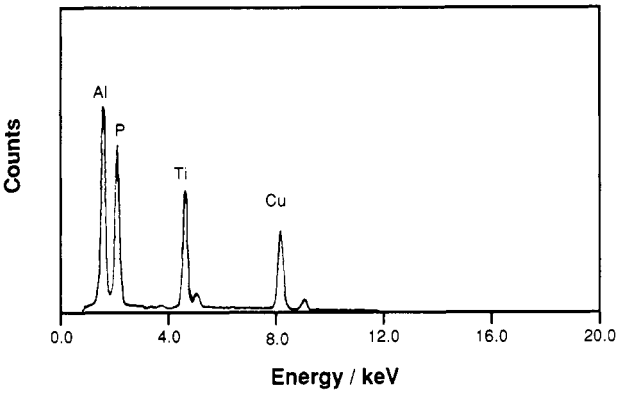

Figure 7. EDX spectrum of aggregate region of micrograph in Figure 5.

are presented in Figures 6 and 7. The Al and P peaks in the spectra are associated with the aluminophosphate molecular sieve VPI-5 and the Cu peak is due to the supporting sample grid. However, Figure 6 shows that the rodlike region contains no titanium whereas a large titanium peak appears in the spectrum of the aggregate region in Figure 7. These results indicate that the titanium dioxide is inhomogeneously loaded into the VPI-5 framework.

Discussion

Several techniques, including X-ray diffraction, ultraviolet reflectance spectroscopy, laser Raman spectroscopy, and transmission electron microscopy, have been used to characterize the formation of titania clusters supported on the aluminophosphate molecular sieve VPI-5. Results from each of these methods give complementary information on the size and location of the clusters in VPI-5, and each technique will be discussed separately.

Synthesis of the supported titania clusters involved calcination of the sample at 673 K. However, the thermal stability of the VPI-5 framework at high temperature depends strongly on the experimental conditions.[18,19] Therefore, evidence of the structural integrity of VPI-5 after the synthesis procedure is necessary. The X-ray diffraction patterns for the calcined and uncalcined TiO_2/VPI-5 samples contained peaks characteristic of the molecular sieve demonstrating that the VPI-5 framework remains intact after calcination at 673 K and that no phase transformations occur. The thermal stability of VPI-5 in this work is in agreement with earlier studies, showing that the molecular sieve, if properly heated under reduced pressure, remains intact at high temperature.[16,17] Since the VPI-5 framework appears to be stable to the titania synthesis procedure, the TiO_2 crystallites can be formed either inside the channels of the molecular sieve or on the external surface. The upper limit on the size of occluded titania is 1.2 nm, the free opening of the VPI-5 channel. Titania supported on the outside of the VPI-5 crystals can grow or sinter to any size with no constraint. Results from X-ray diffraction for both the calcined and uncalcined TiO_2/VPI-5 revealed no peaks other than those associated with the VPI-5 framework. Titania crystallites of 1.2 nm in diameter have very few lattice planes to scatter X-rays so the absence of any titania peaks in the X-ray patterns of the TiO_2/VPI-5 samples is consistent with titania clusters located primarily in the intracrystalline voids of VPI-5.

Further evidence of a small cluster size of the supported titania was obtained from ultraviolet reflectance spectroscopy. The quantum size effect in semiconductor clusters is well-known and can be described as the increase in the optical bandgap energy associated with the decreasing size of semiconductor clusters.[20] This effect is significant mostly for titania cluster sizes smaller than about 10 nm in diameter since the bandgap energies of larger clusters approach the energy of the bulk phase.[21,22] The theory for the cluster size dependence of the bandgap energy has been explained in detail previously and will not be discussed further.[23-25]

Two common phases of bulk titania, rutile and anatase, provided a reference for our TiO_2/VPI-5 sample. The generally accepted bandgap energies of bulk phase rutile and anatase are 3.0 eV (410 nm) and 3.2–3.3 eV (380 nm), respectively, and compare well to 3.05 and 3.28 eV calculated from the UV reflectance spectra in Figure 2 of rutile and anatase powder. However, the bandgap energy measured for the TiO_2/VPI-5 sample is shifted an additional 0.3 eV greater than the energy of unsupported anatase crystals prepared under similar experimental conditions. Evidently, the 0.3 eV shift in bandgap energy for the supported titania results from the size quantization mentioned above.

Anpo et al. report bandgap energies determined from photoluminescence and reflectance spectra of unsupported TiO_2 particles prepared by liquid phase reaction of $TiCl_4$.[21] The smallest particles of anatase in that study were 3.8 nm in diameter and had a bandgap of 3.34 eV which is blue shifted from the bandgap of anatase powder measured in this work but still less than 3.57 eV for TiO_2/VPI-5. Therefore, the significant quantum size effect for the bandgap of TiO_2/VPI-5 indicates that VPI-5 supported titania clusters are less than 3.8 nm in diameter. Yoneyama et al. studied TiO_2 crystallites incorporated in sheet silicates of clay and measured a bandgap of 3.58 eV for microcrystallites with a diameter estimated at 1.5 nm which is very similar to the value found in this study for supported TiO_2.[26] In addition, Krueger et al. recently reported a 0.4-eV blue shift in the TiO_2 UV absorption spectrum of clusters synthesized inside the channels of zeolite L compared to bulk-phase anatase, which is also

(18) Annen, M. J.; Young, D.; Davis, M. E.; Cavin, D. B.; Hubbard, C. R. *J. Phys. Chem.* **1991**, *95*, 1380.
(19) Schmidt, W.; Schuth, F.; Reichert, H.; Unger, K.; Zibrowius, B. *Zeolites* **1992**, *12*, 2.
(20) Henglein, A. *Chem. Rev.* **1989**, *89*, 1861.
(21) Anpo, M.; Shima, T.; Kodama, S.; Kubokawa, Y. *J. Phys. Chem.* **1987**, *91*, 4305.
(22) Miyazaki, S.; Yoneyama, H. *Denki Kagaku* **1990**, *58*, 37.
(23) Brus, L. *Nouv. J. Chim.* **1987**, *11*, 123.
(24) Brus, L. E. *J. Chem. Phys.* **1984**, *80*, 4403.
(25) Wang, Y.; Suna, A.; Mahler, W.; Kasowski, R. *J. Chem. Phys.* **1987**, *87*, 7315.
(26) Yoneyama, H.; Haga, S.; Yamanaka, S. *J. Phys. Chem.* **1989**, *93*, 4833.

similar to the value reported in this work.[11] On the basis of the electron effective mass in TiO_2, they estimated the diameters of the TiO_2/L clusters to be between 1 and 1.5 nm, comparable to the internal dimensions of zeolite L and VPI-5.[11] A similar blue shift in the UV absorption spectrum has also been reported for titania supported inside mordenite.[12] The size of our supported titania clusters can be estimated from the hyperbolic band model of Wang et al.[25] for spherical particles assuming that the effective masses of the photogenerated holes and electrons are $m_h^* = 3m_e$ and $m_e^* = 20m_e$, respectively, (m_e is electron mass).[26,27] On the basis of the bandgaps for bulk-phase anatase and rutile, we estimate that the TiO_2 clusters range from 1.4 to 1.9 nm in diameter, slightly greater than the pore size of the molecular sieve support. This apparent discrepancy can be explained by the titania actually filling the pores in the form of long cylindrical rods instead of spherical clusters. This hypothesis is supported by our TEM/EDX results and will be discussed later. In summary, the UV reflectance characteristics of TiO_2 clusters prepared in VPI-5 are due to size quantization and are consistent with the pore size of the molecular sieve.

The lack of any peaks associated with titania in the X-ray diffraction patterns and the shift of titania bandgap to higher energy are mutually consistent since both results indicate that the titania clusters are most likely inside of the VPI-5 channels. Since the crystal structure of the supported titania could not be determined by X-ray diffraction, the TiO_2/VPI-5 and bulk titania samples were examined by laser Raman spectroscopy. As mentioned earlier, the Raman spectra for bulk-phase reference titanias match previously published results for anatase and rutile. However, interpretation of the spectra from TiO_2/VPI-5 is not as straightforward due to some overlap of peaks from the molecular sieve and titania. Apparently, the low-wavenumber peaks in calcined TiO_2/VPI-5 (432, 310, and 238 cm^{-1}) originate from both TiO_2 and the molecular sieve framework since corresponding peaks are present in the spectra for TiO_2 and pure VPI-5 (the 238-cm^{-1} peak appears after dehydration). However, the two peaks in calcined TiO_2/VPI-5 noted with asterisks at 541 and 670 cm^{-1} are absent from the spectrum of the molecular sieve, so they are attributed solely to the supported titania phase. These titania peaks do not match any of the peaks associated with the reference materials. The titania peaks for TiO_2/VPI-5 are shifted from the bulk phase anatase values to higher wavenumbers by about 25–30 cm^{-1} and are completely different from the peak positions of the bulk-phase rutile. These observations are consistent with the supported TiO_2 microcrystallites having general characteristics of the anatase crystal structure, but the shifts of the Raman peaks to higher wavenumbers indicate modified crystal vibrational modes for the titania molecular sieve. In addition, the peaks appear to be significantly broadened compared to the bulk-phase reference spectra. However, a reliable measurement of the peak broadening is precluded by the large background signal in the region of interest.

One possible explanation for the shifts in the Raman spectrum of TiO_2/VPI-5 compared to that of anatase is suggested by recent results from Raman spectroscopy of nanophase TiO_2 crystallites prepared by gas-phase condensation and oxidation of Ti.[28-30] The rutile peak at 445 cm^{-1} is shifted to lower wavenumbers for oxygen-deficient samples while, conversely, the anatase peak at 145 cm^{-1} (outside the range of the FT Raman instrument used in this work) is shifted to higher wavenumbers for the same oxygen-deficient samples. Additionally, the anatase peak broadened significantly for the oxygen-deficient samples. In summary, peaks in the Raman spectrum of $TiO_{1.88}$ were shifted by 10–20 cm^{-1} and broadened compared to peaks for TiO_2. Similarly, the 30-cm^{-1} shift of the anatase peaks to higher wavenumbers in TiO_2/VPI-5 may result from a severe oxygen deficiency of the supported titania. This idea is also supported by the fact that calcination of the TiO_2/VPI-5 sample was performed in vacuum. If heating the hydrolyzed sample in the absence of dioxygen reduces some of the titanium to Ti^{3+}, then the resulting clusters will be oxygen deficient. Another explanation for the Raman shifts is that the titania crystallites may interact with the molecular sieve framework so that TiO_2 lattice vibrations are greatly modified. Due to the nanometer size of the crystallites, a large fraction of the metal oxide atoms are exposed to the interface and may undergo significant restructuring when in contact with the molecular sieve channels. Therefore, results from the laser Raman study are also consistent with the conclusions derived from the techniques described earlier than the titania microcrystallites supported on VPI-5 are about 1.2 nm in diameter and located primarily inside the channels of the molecular sieve.

An interesting observation in this work is the disappearance of the Raman peak at ~1100 cm^{-1} in Figure 4a for calcined TiO_2/VPI-5 compared to the other samples. Damage to the sample from laser exposure is eliminated as a cause for the disappearance of the high-wavenumber band because only 200 scans were averaged to produce Figure 4a compared to 1500 scans for Figure 4b. Since X-ray diffraction (Figure 1) revealed that the molecular sieve structure remains intact after calcination, an explanation for the disappearance of the 1100-cm^{-1} band after calcination is not clear at this time.

Transmission electron microscopy and EDX spectroscopy were used to determine how the titania was distributed throughout the sample. As seen by the two regions of solid sample in Figure 5, two types of material are present in the sample. Results from EDX spectroscopy revealed that titanium is located exclusively in the aggregate region instead of being distributed homogeneously throughout the material. Elemental analysis of the overall sample showed that the average titanium loading was 5.06 wt %. Since the void volume of VPI-5 measured by neopentane adsorption is about 0.15 $cm^3\ g^{-1}$ [31] and the bulk density of anatase is 3.90 g cm^{-3}, approximately 16% of the total void volume of VPI-5 is filled by titania. However, results from TEM and EDX spectroscopy show an inhomogeneous loading, suggesting that some regions of the sample may contain VPI-5 completely filled with titania while other regions lack titania. The atomic ratios of Al, P, and Ti, estimated from the EDX spectra of the hydrolyzed sample in Figure 7 and also the calcined TiO_2/VPI-5 sample (not shown) are consistent with titania nearly filling the channels but not exceeding the capacity of fully loaded VPI-5. Therefore, the titania is most likely located *inside* the VPI-5 framework and may exist either as long rods that fill the channels or as many separate clusters in close proximity in the channel. The techniques used in this work cannot distinguish between the two cases.

(27) Kasinski, J. J.; Gomez-Jahn, L. A.; Faran, K. J.; Gracewski, S. M.; Dwayne Miller, R. J. *J. Chem. Phys.* **1989**, *90*, 1253.
(28) Melendres, C. A.; Narayanasamy, A.; Maroni, V. A.; Siegel, R. W. *J. Mater. Res.* **1989**, *4*, 1246.
(29) Parker, J. C.; Siegel, R. W. *J. Mater. Res.* **1990**, *5*, 1246.
(30) Parker, J. C.; Siegel, R. W. *Appl. Phys. Lett.* **1990**, *57*, 943.
(31) Davis, M. E.; Montes, C.; Hathaway, P. E.; Arhancet, J. P.; Hasha, D. L.; Garces, J. M. *J. Am. Chem. Soc.* **1989**, *111*, 3919.

These results emphasize the importance of complementing experimental techniques that measure properties averaged over a macroscopic sample with techniques capable of microscale resolution. For example, the scattering and spectroscopic techniques used here were incapable of detecting the TiO_2/VPI-5 sample inhomogeneity observed by TEM and EDX. If the X-ray diffraction peaks in Figure 1b are due solely to scattering from the rodlike regions of the sample, then the influence of occluded titania on the molecular sieve framework stability remains inconclusive. The overall conclusions of this work are significant for those researchers working with supported semiconductor clusters since structure and property measurements of the final system derived from macroscale techniques may be misinterpreted without additional materials characterization on a microscale.

Acknowledgment is made to the donors of The Petroleum Research Fund, administered by the American Chemical Society, for support of this research (ACS-PRF 24446-G5). Suk Bong Hong and James Howe are gratefully acknowledged for their aid with laser Raman spectroscopy and transmission electron microscopy, respectively. Mark Davis is also acknowledged for providing the VPI-5 used in this work.

Registry No. TiO_2, 13463-67-7.

New Complementary Electrochromic System Based on Polypyrrole–Prussian Blue Composite, a Benzylviologen Polymer, and Poly(vinylpyrrolidone)/Potassium Sulfate Aqueous Electrolyte

Nicholas Leventis* and Young C. Chung

Molecular Displays, Inc., 38 Smith Place, Cambridge, Massachusetts 02138

Received July 7, 1992. Revised Manuscript Received September 29, 1992

A new redox complementary electrochromic system is described that is based on electrode surface confined electrochromic polymers. Emphasis is given on the synergism achieved with the implementation of the complementary counter electrode technology: polypyrrole–prussian blue (PP-PB) composite was employed as the oxidatively colored material, and a viologen polymer (pBPQ) derived from *N,N'*-bis[*p*-(trimethoxysilyl)benzyl]-4,4'-bipyridinium dichloride (BPQ) was used as the reductively colored material. A viscous aqueous solution of poly(vinylpyrrolidone) (PVP)/K_2SO_4 was used as the electrolyte. To our knowledge, this is the first example of a complementary electrochromic system where *both* electrochromic materials are electrode surface confined electrochromic polymers. In this paper, the electrochromic materials and the electrolyte are characterized individually, and their properties are discussed in relation to the performance of the electrochromic system. On the basis of the electrochromic system mentioned above, two terminal transmissive and reflective 4 in. × 4 in. electrochromic devices are able to switch from colorless ($A_{400-800} \simeq 0.15$–0.25) to blue ($A_{650} \simeq 1.35$) in about 3–5 s, with the application of 0.8–0.9 V across the two electrodes.

Introduction

Upon oxidation or reduction, certain redox-active materials undergo quite significant changes in their optical absorption spectrum. This phenomenon is called electrochromism, and such materials are called electrochromic.[1,2] Consequently, considerable attention is being focused currently on electrochromism, due to its potential application to light modulation.[1] For this purpose, electrochromic materials are incorporated into electrochromic devices, which are chemical systems composed of one or more such materials and an electrolyte, all confined in a two-electrode electrochemical cell with at least one of its electrodes clearly visible from outside of the cell.

In this paper emphasis is given on surface-confined polymeric electrochromic materials, and the synergism achieved with the implementation of the complementary counterelectrode technology. We report the preparation and characterization of electrode surface confined films of polypyrrole–prussian blue (PP-PB) composite, and we demonstrate functional self-contained reflective and transmissive electrochromic devices incorporating this electrochromic material. A viologen polymer derived from *N,N'*-bis[*p*-(trimethoxysilyl)benzyl]-4,4'-bipyridinium dichloride (BPQ)[3] is employed as the electrochromic material redox complementary to PP-PB, while a viscous aqueous solution of poly(vinylpyrrolidone) (PVP)/K_2SO_4 is incorporated as the electrolyte.

Ideally, an electrochromic device includes two electrochromic materials with "complementary" properties.[4] The first electrochromic material undergoes a colorless-to-colored transition oxidatively, while simultaneously the second electrochromic material undergoes the same color transition reductively. This technology has two distinct advantages. First, the long-term stability of the electrochromic cell is greatly enhanced by preventing any electrolytic decomposition of the electrolyte since both a source and a sink of electrons are provided within the same system simultaneously. Second, the two electrochromic materials change color simultaneously, enhancing the contrast between the colored and colorless states.

Depending on the relative location of the two electrochromic materials within the electrochromic devices, three main types of such devices exist:[4] (a) the solution phase,

* Address correspondence to this author.

(1) Grover, D. J. *Display* **1988**, *9*, 163 (the entire issue).
(2) Oi, T. *Annu. Rev. Mater. Sci.* **1986**, *16*, 185.
(3) Dominey, R. N.; Lewis, T. J.; Wrighton, M. S. *J. Phys. Chem.* **1983**, *87*, 5345.
(4) Hamada, H.; Yano, K.; Take, H.; Inami, Y.; Matsuura, M.; Wada, T. *Displays* **1983**, *4*, 221.

0897-4756/92/2804-1415$03.00/0